On the Fermionic Shadow Wave Function and novel attempts to solve its sign problem

Francesco Calcavecchia[1], Francesco Pederiva[2] and Thomas D. Kühne[1,3]

[1] *Institut of Physical Chemistry, Johannes Gutenberg-University Mainz, Staudinger Weg 9, D-55128 Mainz, Germany*

[2] *Dipartimento di Fisica, University of Trento, via Sommerive 14, I-38050 Povo, Trento, Italy*

[3] *Center for Computational Sciences, Johannes Gutenberg-University Mainz, Staudinger Weg 9, D-55128 Mainz, Germany*

(Received June 11th, accepted June 30th, published online July 9th 2011

We present the Fermionic Shadow Wave Function in the context of variational quantum Monte Carlo for disordered systems. Using the example of liquid ^{3}He it is demonstrated that this allows for very accurate calculations, but due to its sign problem only for small systems. For this reason two novel methods are proposed that in principle solve the associated sign problem, but do not allow for realistic simulations yet.

The difficulty to solve the Schrödinger equation for many interacting particles is due to the fact that it is in general impossible to analytically solve it for more than a few particles. Variational Monte Carlo (VMC) [1] is a stochastic method which allows to find the ground-state solution of the many-body Schrödinger equation. The main ideas underlying VMC are the application of the variational principle and the use of importance sampling Monte Carlo to efficiently evaluate the high-dimensional integrals of many different expectational values and in particular the energy [1]

$$E = \frac{\int dR\, \psi^*(R) H \psi(R)}{\int dR\, \psi^*(R)\psi(R)}\,. \tag{1}$$

Since many-particle correlation effects are included by the use of a so-called trial wave function, VMC is substantially more accurate than commonly used mean field methods and permits to treat even strongly correlated systems. From the outset the exact trial wave function is unknown and needs to be approximated. However, due to the fact that adding a simple correlation function, such as the Jastrow correlation factor, permits to recover most of the dynamic correlation, in many cases VMC gives excellent results.

Here we consider the Shadow Wave Function (SWF), first introduced by Vitiello, Runge and Kalos [2], as our trial function. In particular, since the SWF allows to describe all possible condensed phases (gas, liquid and solid) and even phase coexistence [3] within the same functional form. As a consequence, it is for instance possible to simulate a solid without explicitly defining its crystal structure, which instead emerges from the calculation. In fact, with the SWF it is even feasible to describe inhomogeneous systems [4–6]. Moreover, the SWF has further very appealing properties, e.g. it introduces correlation of any order and obeys a strong similitude with the exact bosonic ground state wave function.

The general form of the SWF takes the form

$$\psi_{\text{SWF}}(R) \equiv \psi_p(R) \int dS\, \Xi(R,S)\, \psi_s(S)\,, \tag{2}$$

where S are auxiliary degrees of freedom called shadows, $\psi_p(R)$ and $\psi_s(S)$ are Jastrow functions that describe the correlation between the particles and between the shadows respectively, while $\Xi(R,S)$ is a kernel that correlates the particles with their shadows. Neglecting, for the moment, the requirement of antisymmetry necessitated by the Pauli exclusion principle, typical choices are

$$\psi_p(R) = e^{-\frac{1}{2}\sum_{i<j} u_{pp}(r_{ij})} \tag{3a}$$

$$\psi_s(S) = e^{-\sum_{i<j} u_{ss}(s_{ij})} \tag{3b}$$

$$\Xi(R,S) = e^{-\sum_{i=1}^{N_p} u_{ps}(|\mathbf{r}_i - \mathbf{s}_i|)}\,, \tag{3c}$$

where u_{pp}, u_{ss} and u_{ps} are the so-called two-body pseudopotentials, since they have a role similar to the potential in the Boltzmann distribution. Although it is possible to include three-body and even higher order terms, for the sake of simplicity they are not considered here. In any case the SWF not only maintains the translational properties of the gas and liquid phases, but through the kernel also enables the necessary localization to accurately describe the solid phase. In fact, for densities at which the system is experimentally found to be in the the solid phase, the variational optimized parameters yields a localization of the shadows in the correct crystal structure. The real degrees of freedom are in turn localized near the corresponding shadows by the kernel.

In a few studies, the SWF has been successfully applied to bosonic systems, in which the wave function is non-negative [3, 7–10]. However, due to the aforementioned antisymmetry requirement, the extension to fermionic systems is nontrivial and gives rise to a sign problem. Generally, an efficient and rigorous method to simulate fermionic systems therefore remains an open and most challenging problem.

The extension of the SWF to fermionic systems, where the wave function is real but equally positive and negative, is established in Section 1. The origin and impact of the sign problem will be exposed in Section 2, while in Sections 3 and 4 we are going to present and discuss in depth two novel attempts to solve it.

1 The Shadow Wave Function for Fermions

As fermions obey Fermi-Dirac statistics, an antisymmteric version of the SWF is required, that must change sign upon interchange of any two fermions in order to comply with the Pauli exclusion principle.

The simplest way to achieve this, is to adjoin the Jastrow correlation factor with a Slater Determinant (SD) that depends on the particle positions R. We will call this the Antisymmetric Shadow Wave Function (ASWF) [8]

$$\psi_{\text{ASWF}}(R) \equiv \det(\phi_\beta(\mathbf{r}_\alpha))\, \psi_p(R) \int dS\, \Xi(R,S)\, \psi_s(S)\,, \tag{4}$$

where $\phi_\beta(\mathbf{r}_\alpha)$ are the orbitals that represent the SD. In order to preserve the translational symmetry of the wave function, which is one of the many appealing properties of the SWF, plane wave orbitals are the natural choice.

Another possibility is to introduce a SD built up of orbitals as a function of shadow positions S. The resulting Fermionic Shadow Wave Function (FSWF) then reads as:

$$\psi_{\text{FSWF}}(R) = \psi_p(R) \int dS\, \Xi(R,S)\, \det(\phi_\beta(\mathbf{s}_\alpha))\, \psi_s(S)\,. \tag{5}$$

It is possible to demonstrate that, just as the ASWF, the FSWF is antisymmetric upon particles exchange [11]. But since the latter furthermore provides [12] (i) a closer similitude with the projection onto the exact fermionic ground state (no one actually knows how the propagator on the lowest antisymmetric state behaves), (ii) the correct asymptotic nodal structure and (iii) naturally includes backflow effects [13], the FSWF rather than the ASWF is to favor.

As can be seen in Table 1, applying the FSWF to the liquid phase ^{3}He provides much improved variational energies, even though only for a rather

[1] We use the notation $R \equiv (\mathbf{r}_1, \mathbf{r}_2, \ldots \mathbf{r}_N)$ and $S \equiv (\mathbf{s}_1, \mathbf{s}_2, \ldots \mathbf{s}_N)$.

[2] We consider an unpolarized 3D system of ^{3}He at a density equal to 0.016588 Å^{-3} (liquid phase) using the Aziz potential HFDHE2 [14, 15] and periodic boundary conditions in order to mimic an essentially infinite system. We remark that whenever a SD with orbital made up of plane waves is used, the occurrence of a drift (i.e. $\sum_\beta \mathbf{k}_\beta \neq 0$) as well as anisotropy has to be taken explicitly into account. The simplest remedy is to consider only magic numbers for N, i.e. numbers that fill the momenta shell. For a 3D system they are: 1, 7, 19, 27, 33, ...

small system with $N = 38$ particles and with an admittedly larger statistical uncertainty. [2] In fact, as we are going to explain in detail in the next section, the FSWF entails a serious sign problem that makes it essentially impossible to obtain reliable results whenever $N > 38$. This limitation on the size of the system not only reduces the applicability, but also the reliability of the FSWF, due to fairly large finite-size effects. Therefore, it would be desirable to solve, or at least alleviate, the sign problem and allow for even more accurate simulations with many more particles. In order to approximately compare the various energies for different values of N, from now on, we shall refer to the energy per particle, denoted as $\mathcal{E}$.

Trial Function	$\mathcal{E}$	N
J-SD	-1.004 ± 0.006 K	66
ASWF	-1.222 ± 0.006 K	66
FSWF	-1.966 ± 0.035 K	38

Table 1: The energy per particle of liquid ^{3}He is denoted by $\mathcal{E}$, which is obtained by VMC calculations using different trial wave functions. The number of particles is indicated by N, while the Jastrow-SD (J-SD) trial wave function is defined as $\psi_{\text{J-SD}} \equiv \det(\phi_\beta(\mathbf{r}_\alpha))\,\psi_p(R)$, where $\phi_\beta(\mathbf{r}_\alpha)$ are plane waves.

2 The Sign Problem of the Fermionic Shadow Wave Function

Applying the FSWF causes a serious challenge in the evaluation of the energy, which is indispensable to employ the variational principle. Usually the energy can be estimated by

$$E \simeq \frac{1}{M}\sum_{i=1}^{M} E^{loc}(R_i)\,, \tag{6}$$

where $E^{loc}(R_i) = \frac{H\psi(R_i)}{\psi(R_i)}$ is the so-called local energy and M the number of sampling points. The positions of the particles R_i are sampled from the probability density function (pdf) $\psi^2(R)$, where ψ is the trial wave function. As a consequence, the necessary positiveness of $\psi^2(R)$ is satisfied by definition.

Introducing further the shadows, the energy is evaluated as [3]

$$E = \frac{\int dR\, dS_1 dS_2\, \psi_{\text{SWF}}(R,S_1) H \psi_{\text{SWF}}(R,S_2)}{\int dR\, dS_1 dS_2\, \psi_{\text{SWF}}(R,S_1)\psi_{\text{SWF}}(R,S_2)}\,, \tag{7}$$

so that the corresponding energy estimator can be written as

$$E \simeq \frac{1}{M}\sum_{i=1}^{M}\frac{1}{2}(E^{loc}(R_i,S_{1\,i}) + E^{loc}(R_i,S_{2\,i}))\,, \tag{8}$$

where R_i, $S_{1\,i}$ and $S_{2\,i}$ are sampled from the pdf $\psi_{\text{SWF}}(R,S_1) \times \psi_{\text{SWF}}(R,S_2)$. The average between the S_1 and S_2 contributions to E^{loc} is introduced in order to accelerate the convergence. Now the positiveness of the sampled function is no more obviously satisfied, since the wave function is evaluated using two different shadows. It straightforward to see that this problem arises for ψ_{FSWF}, because the SD uses the shadow positions, whereas this is not the case for ψ_{ASWF}. Therefore, it is not possible to sample directly from the pdf $\psi_{\text{FSWF}}(R,S_1) \times \psi_{\text{FSWF}}(R,S_2)$.

However, it is possible to overcome this problem by a simple modification, that is to sample from the pdf $|\psi_{\text{FSWF}}(R,S_1) \times \psi_{\text{FSWF}}(R,S_2)|$ and to introduce the weights

$$\omega_i = \frac{\psi_{\text{FSWF}}(R_i,S_{1\,i})\psi_{\text{FSWF}}(R_i,S_{2\,i})}{|\psi_{\text{FSWF}}(R_i,S_{1\,i})\psi_{\text{FSWF}}(R_i,S_{2\,i})|} = \pm 1\,. \tag{9}$$

The modified energy estimator then reads as

$$E \simeq \frac{\sum_{i=1}^{M}\frac{\omega_i}{2}(E^{loc}(R_i,S_{1\,i}) + E^{loc}(R_i,S_{2\,i}))}{\sum_{i=1}^{M}\omega_i}\,. \tag{10}$$

Since the sign is now carried by ω_i, the sum in Eq. 10 may be very slowly converging. For disordered systems such as liquid ^{3}He studied here this is particularly severe.

[3] We use the obvious notation $\psi_{\text{SWF}}(R,S) = \psi_p(R)\,\Xi(R,S)\,\psi_s(S)$.

[4] Since the Central Limit Theorem requires independent random samples.

Here we have chosen to use the pseudopotentials

$$u_{pp}(r_{ij}) = (\frac{b}{r_{ij}})^5 \tag{11a}$$

$$u_{ss}(s_{ij}) = c_1 V(c_2 s_{ij}) \tag{11b}$$

$$u_{ps}(|\mathbf{r}_i - \mathbf{s}_i|) = C|\mathbf{r}_i - \mathbf{s}_j|^2\,, \tag{11c}$$

where V is the Aziz potential used in the Hamiltonian, while b, c_1, c_2 and C are variational parameters.

To evaluate the mean value and its unbiased error bar, we have divided the data into n_{block} disjoint blocks each with its corresponding average value E_j^{block}. It is then possible to calculate the average and the error bar in the following way:

$$\langle E\rangle_{\text{block}} = \frac{1}{n_{\text{block}}}\sum_{j=1}^{n_{\text{block}}} E_j^{\text{block}}\,, \tag{12a}$$

$$\sigma^2_{\text{block}} = \frac{1}{n_{\text{block}}}\sum_{j=1}^{n_{\text{block}}}\left(E_j^{\text{block}} - \langle E\rangle_{\text{block}}\right)^2\,. \tag{12b}$$

This is the so-called blocking technique [16] to get an estimate for the error bar at the presence of serial correlation between successive samples. Otherwise, evaluating the variance in the straightforward way would provide an underestimated small error bar, due to serial correlation of successive data points, which artificially reduces the variance[4]. Using the blocking technique and given that $\frac{M}{n_{\text{block}}}$ is high enough, there is no serial correlation between the E_j^{block} values anymore, so that σ can be correctly estimated.

Plotting σ_{block} as a function of n_{block} and assuming that M is sufficiently large, for the correct estimate of the error a plateau is observed. We remark that in general $\langle E\rangle_{\text{block}}$ is not equal to E, but as long as M is large enough, each E_j^{block} will be very close to E, so that eventually E agrees with $\langle E\rangle_{\text{block}}$ within one standard deviation.

n_{block}	$\langle\mathcal{E}\rangle_{\text{block}}$	$\langle\mathcal{E}_{kin}\rangle_{\text{block}}$	$\langle\mathcal{E}_{pot}\rangle_{\text{block}}$
4	-2.07 K	12.20 K	-14.26 K
8	-12.12 K	8.21 K	-20.33 K
12	-1.60 K	13.89 K	-15.49 K
16	-2.36 K	11.57 K	-13.93 K
24	-2.58 K	16.18 K	-18.76 K

Table 2: The mean local energies per particle for the liquid phase of ^{3}He with respect to different number of blocks. All results were obtained using ψ_{FSWF} averaged over $M = 10^8$ sampling points and $N = 66$.

Looking at Table 2 it is apparent that the FSWF exhibits very large fluctuations in $\langle\mathcal{E}\rangle_{\text{block}}$ for different n_{block}. From this it follows that it is impossible to determine a reliable mean value and an associated error bar, which clearly characterizes the sign problem of the FSWF. Figs. 1 and 2 demonstrate that the sign problem is due to the alternating sign of the weights, since the fluctuations of the local energies are of the same magnitude that we have found using the ASWF.

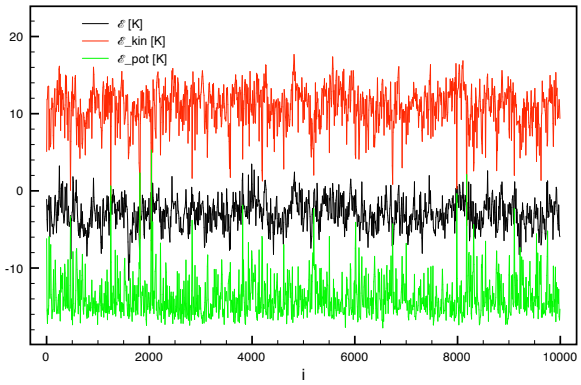

Figure 1: The instantaneous local energies per particle $\mathcal{E}^{loc}$, $\mathcal{E}^{loc}_{kin}$ and $\mathcal{E}^{loc}_{pot}$ for 66 particles of liquid ^{3}He using ψ_{FSWF}.

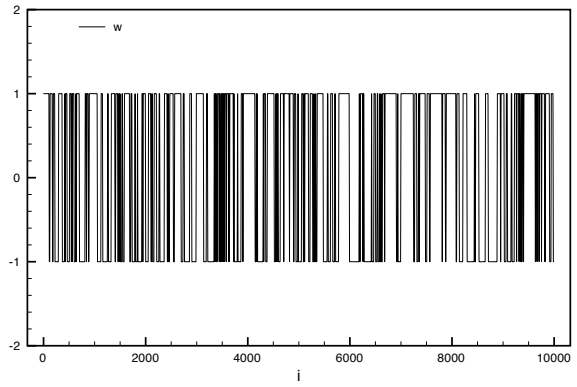

Figure 2: The instantaneous weights ω_i (see Eq. 9), as obtained using ψ_{FSWF} for the liquid phase of ^{3}He with $N = 66$.

It is important to emphasize, that the sign problem of the FSWF differs from the infamous fermion sign problem of Green's Function [17] or Diffusion Monte Carlo [18], because in principle it should be possible to find a viable solution to eliminate the former. Nevertheless, the convergence is drastically reduced, so that in many cases (like the one that we have just illustrated) it is practically impossible to get reliable results.

3 The Antithetic Shadow Approach

A first attempt [12] to solve the sign problem is to introduce new auxiliary shadows, which will carry the opposite sign with respect to the original ones. The idea is that this will lead to a direct summation of opposite contributions and eventually to a faster convergence. From now on we will indicate the original shadows as S^+ and the auxiliary ones as S^-.

It can be easily proved that in one dimension

$$e^{-c(x-s^+)^2} = \frac{\sqrt{\sigma_1^2+\sigma_2^2}}{\sqrt{2\pi}\sigma_1\sigma_2}\int ds^- \, e^{-\frac{(x-s^+)^2}{2\sigma_1^2}} \times e^{-\frac{(x-s^-)^2}{2\sigma_1^2}} e^{-\frac{(s^++s^--2x)^2}{2\sigma_2^2}}, \quad (13)$$

where σ_1 and σ_2 must satisfy the relationship

$$c = \frac{2\sigma_1^2+\sigma_2^2}{2\sigma_1^2\left(\sigma_1^2+\sigma_2^2\right)}. \quad (14)$$

It is straightforward to adopt this identity within the FSWF, replacing the kernel $\Xi(R,S)$ with [5]

$$\Xi(R,S^+,S^-) = e^{-\sum_{i=1}^N\left[\frac{(\mathbf{s}_i^+-\mathbf{r}_i)^2+(\mathbf{s}_i^--\mathbf{r}_i)^2}{2\sigma_1^2}+\frac{(\mathbf{s}_i^++\mathbf{s}_i^--2\mathbf{r}_i)^2}{2\sigma_2^2}\right]}. \quad (15)$$

Setting $\sigma_2 \ll 1$, S^- will be almost exactly opposite to S^+ with respect to R. We note that for symmetry reasons it is possible to write

$$\psi_{\text{FSWF}} = \psi_p(R)\int dS^+dS^- \,\Xi(R,S^+,S^-) \times \left(\det(\phi_\beta(\mathbf{s}^+{}_\alpha))\,\psi_s(S^+)+\det(\phi_\beta(\mathbf{s}^-{}_\alpha))\,\psi_s(S^-)\right). \quad (16)$$

In this way, S^- will almost always carry the opposite sign of S^+ whenever R will be close to the nodal surface of the SD, which is exactly when the sign problem arises. If this is the case, the sum of two opposite contributions, that explicitly appears in the wave function, will give rise to a much faster convergence of the average. For this reason we will call S^- an antithetic shadow and the corresponding new expression for the FSWF Antithetic Fermionic Shadow Wave Function, denoted as ψ_{aFSWF}.

Using ψ_{aFSWF}, the best results are obtained by sampling from the pdf defined as the absolute value of

$$\mathcal{P} = \psi_p^2(R)\,\Xi(R,S_1^+,S_1^-)\,\Xi(R,S_2^+,S_2^-) \times \left(\det(\phi_\beta(\mathbf{s}_{\mathbf{1}}^+{}_\alpha))\,\psi_s(S_1^+)\,\det(\phi_\beta(\mathbf{s}_{\mathbf{1}}^-{}_\alpha))\,\psi_s(S_1^-)\right) \times \left(\det(\phi_\beta(\mathbf{s}_{\mathbf{2}}^+{}_\alpha))\,\psi_s(S_2^+)\,\det(\phi_\beta(\mathbf{s}_{\mathbf{2}}^-{}_\alpha))\,\psi_s(S_2^-)\right) \quad (17)$$

[5] Normalization factors are always omitted.

and hence

$$\omega_i = \frac{\mathcal{P}}{|\mathcal{P}|}\left(\frac{1}{\det(\phi_\beta(\mathbf{s}_{\mathbf{1}}^+{}_\alpha))\,\psi_s(S_1^+)}+\frac{1}{\det(\phi_\beta(\mathbf{s}_{\mathbf{1}}^-{}_\alpha))\,\psi_s(S_1^-)}\right) \times \left(\frac{1}{\det(\phi_\beta(\mathbf{s}_{\mathbf{2}}^+{}_\alpha))\,\psi_s(S_2^+)}+\frac{1}{\det(\phi_\beta(\mathbf{s}_{\mathbf{2}}^-{}_\alpha))\,\psi_s(S_2^-)}\right). \quad (18)$$

At first sight it might appear that with our antithetic shadow approach substantial progress has been made towards solving the sign problem. Unfortunately, for $\sigma_2 \ll 1$ the Gaussian

$$e^{-\frac{(s^++s^--2x)^2}{2\sigma_2^2}} \quad (19)$$

becomes very narrow and therefore involves large fluctuations in the kinetic energy, that gets even more severe as σ_2 decreases. This behavior is evident by noticing the magnitude of the kinetic energy fluctuations of Fig. 3, in particular when comparing it with Fig. 1.

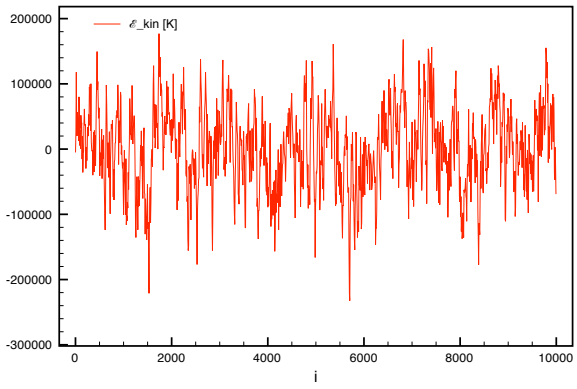

Figure 3: The instantaneous local kinetic energy per particle $\mathcal{E}_{kin}^{loc}$ for 66 particles of ^{3}He in the liquid phase using ψ_{aFSWF} with $\sigma_2 \approx 0.01$ Å.

n_{block}	$\sigma_2 \approx 0.5$ Å	$\sigma_2 \approx 0.01$ Å	$\sigma_2 \approx 0.001$ Å
4	25.6 K	1040.5 K	−4688389.6 K
8	−1.0 K	899.8 K	−157032.5 K
12	118.8 K	262.2 K	−1501955.0 K
16	−6.9 K	−851.0 K	−863894.5 K
24	1.4 K	−1777.0 K	13943120.4 K

Table 3: The mean energy per particle $\langle\mathcal{E}\rangle_{\text{block}}$ of liquid ^{3}He. The results were obtained for $N = 66$ by sampling ψ_{aFSWF} with $M = 10^7$.

Looking at the total energies of Table 3 it may seem that, using the antithetic shadow approach, the results are even worse than before, notably when σ_2 is small. Nevertheless, the sign problem is indeed substantially reduced as demonstrated by Fig. 4. In fact, the comparison with Fig. 2 clearly exhibits a stabilization of the sign. As a consequence, the evaluation of the potential energy is indeed dramatically improved, as given in Table 4 and in contrast with Fig. 1.

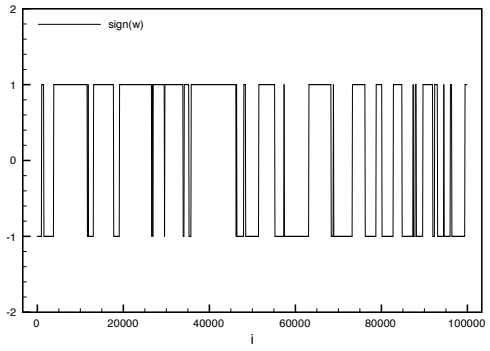

Figure 4: The instantaneous weights ω_i (see Eq. 18) of liquid ^{3}He with $N = 66$ using ψ_{aFSWF} with $\sigma_2 \approx 0.01$ Å.

n_{block}	$\sigma_2 \approx 0.5$ Å	$\sigma_2 \approx 0.01$ Å	$\sigma_2 \approx 0.001$ Å
4	-16.63 K	-16.12 K	-16.42 K
8	-15.88 K	-15.91 K	-16.45 K
12	-16.28 K	-15.94 K	-17.09 K
16	-16.75 K	-16.12 K	-16.35 K
24	-15.98 K	-17.20 K	-12.05 K

Table 4: The mean potential energy per particle $\langle \mathcal{E}_{pot} \rangle_{\text{block}}$ using ψ_{aFSWF} with $M = 10^7$ and $N = 66$. When σ_2 becomes too small the results deteriorate because of the increasing autocorrelation between the samplings points.

Even though using the antithetic approach in its current form it is not possible to directly evaluate the energy and optimize ψ_{aFSWF}, it anyhow alleviates the sign problem and allows to reliably evaluate all observables that do not imply any derivatives of the wave function.

Finally, we wish to point out an aspect of our approach that needs to be improved in the future. The pdf of Eq. 17 that we used originates from a simple mathematical manipulation in order to sample from a product rather than a sum of functions, since the latter can not be effectively sampled [11]. However, this entails that the SD may become arbitrarily close to zero and thus the corresponding weights unbounded. The fact that the variance of the weights is therefore infinite necessitates an improved sampling function.

4 The Artificial Shadow Correlation Method

As an alternative scheme to solve the sign problem we propose another method, which forces the shadows S_1 and S_2 to almost overlap so that the product of the two corresponding SD will be always positive. In order to achieve this, we insert the artificial term $e^{-k \sum_{i=1}^{N} (\mathbf{s}_{1\,i} - \mathbf{s}_{2\,i})^2}$, that correlates S_1 with S_2. We therefore call this technique the artificial shadow correlation method. However, inserting this artificial term into Eq. 7 exhibit a systematic bias in the energy due to the non-physical nature of the additional expression, which is only present to avoid the sign problem. Nevertheless, considering the energy per particle $\mathcal{E}(k)$ as a function of the fictitious parameter k, it is still possible to estimate the energy. Fitting $\mathcal{E}(k)$ for different k values with an arbitrary function admits to extrapolate to $k = 0$, where the additional term is identical zero and the correct energy $\mathcal{E}(k = 0)$ is recovered. However, as displayed in Fig. 5 the accuracy of the energy estimation crucially depends on the particular function to extrapolate $\mathcal{E}(k)$ to $k = 0$.

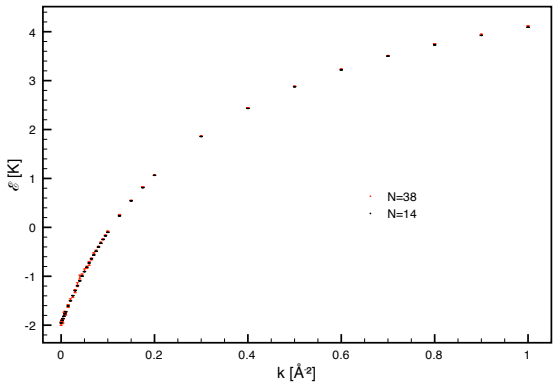

Figure 5: The energy per particle $\mathcal{E}(k)$ with respect to the fictitious parameter k.

In order to demonstrate this approach we fit $\mathcal{E}(k)$ using the functions

$$f_2(k) = \frac{A\,k^2 + B\,k + C}{k^2 + D\,k + E}, \tag{20a}$$

as well as

$$f_3(k) = \frac{A\,k^3 + B\,k^2 + C\,k + D}{k^3 + E\,k^2 + F\,k + G}\,. \tag{20b}$$

We find that both functions pass Pearson's chi-square test for both $N = 14$ and $N = 38$. However, we were not able to obtain reliable results for $N = 66$ whenever $k < 0.4$ Å^{-2}. That is why in Table 5 only results for $N = 14$ and $N = 38$ with $k > 0.4$ Å^{-2} are reported and compared to the values of plain FSWF calculations. While $f_2(k)$ is not flexible enough to yield satisfactory results, $f_3(k)$ may constitute an improvement. However, due to the large number of fitting parameters that needs to be determined, at this stage the statistical uncertainty is much too high to obtain any meaningful result.

N	$\mathcal{E}$	$f_2(k=0)$	$f_3(k=0)$
14	-1.9535 ± 0.0023 K	-1.89 ± 0.19 K	-2.0 ± 3.1 K
38	-1.966 ± 0.035 K	-1.78 ± 0.11 K	-2.2 ± 2.9 K

Table 5: The energy per particle $\mathcal{E}$, as obtained by direct FSWF simulations and by fitting $f_2(k)$ as well $f_3(k)$, where 0.4 Å$^{-2} < k < 100$ Å^{-2}, using 25 points each with an error bar of $\sim 10^{-3}$ K.

5 Conclusions

The extension of the SWF to fermionic systems, which has been outlined here, entails a serious sign problem that makes it impractical - barring additional technical improvements - to simulate the liquid or any other non-crystalline phase of a many particle system. We have presented two novel methods to solve this problem, the antithetic shadow approach and the artificial shadow correlation method. The former is a viable approach to alleviate the sign problem and allows to calculate all expectation values that do not depend on the derivative of the wave function, such as the potential energy. However, it does not permit to calculate the kinetic energy and therefore in particular not the total energy. Nevertheless, our second method may represent an interesting avenue to facilitate exactly that and eventually solve the sign problem. Unfortunately, in its present form the extrapolation to $k = 0$ is simply not accurate enough.

Further advances that we are currently investigating, as well as a conclusive study on liquid ^{3}He will be presented elsewhere.

6 Acknowledgments

We would like to thank M. H. Kalos for numerous valuable discussions. FC gratefully acknowledges financial support from the Graduate School of Excellence MAINZ. Part of the computations has been performed on the HPC facility of the Department of Physics, University of Trento.

References

[1] W. L. McMillan, Phys. Rev. **138**, A442 (1965).

[2] S. Vitiello, K. Runge, and M. H. Kalos, Phys. Rev. Lett. **60**, 1970 (1988).

[3] F. Pederiva, A. Ferrante, S. Fantoni, and L. Reatto, Phys. Rev. Lett. **72**, 2589 (1994).

[4] F. Pederiva, G. V. Chester, S. Fantoni, and L. Reatto, Phys. Rev. B **56**, 5909 (1997).

[5] F. Operetto and F. Pederiva, Phys. Rev. B **69**, 024203 (2004).

[6] L. Dandrea, F. Pederiva, S. Gandolfi, and M. H. Kalos, Phys. Rev. Lett. **102**, 255302 (2009).

[7] S. A. Vitiello, K. J. Runge, G. V. Chester, and M. H. Kalos, Phys. Rev. B **42**, 228 (1990).

[8] F. Pederiva, S. A. Vitiello, K. Gernoth, S. Fantoni, and L. Reatto, Phys. Rev. B **53**, 15129 (1996).

[9] F. Operetto and F. Pederiva, Phys. Rev. B **75**, 064201 (2007).

[10] S. A. Vitiello, L. Reatto, G. V. Chester, and M. H. Kalos, Phys. Rev. B **54**, 1205 (1996).

[11] F. Calcavecchia, Master's thesis, Universitá degli studi di Trento (2010).

[12] M. H. Kalos and L. Reatto, in *Progress in Computational Physics of Matter*, edited by L. Reatto and F. Manghi (World Scientific, Singapore, 1995).

[13] R. P. Feynman and M. Cohen, Phys. Rev. **102**, 1189 (1956).

[14] R. A. Aziz, V. P. S. Nain, J. S. Carley, W. L. Taylor, and G. T. McConville, J. Chem. Phys. (1979).

[15] S. A. Sofianos, S. A. Rakityansky, and S. E. Massen, Phys. Rev. A **60**, 337 (1999).

[16] M. H. Kalos and P. A. Whitlock, *Monte Carlo Methods* (Wiley-VCH, Weinheim, 2008).

[17] M. H. Kalos, D. Levesque, and L. Verlet, Phys. Rev. A **9**, 2178 (1974).

[18] D. M. Ceperley and B. J. Alder, Phys. Rev. Lett. **45**, 566 (1980).